Desalination and Water Treatment
www.deswater.com
18 (2010) 46–60
June
1944-3994 / 1944-3986
doi: 10.5004/dwt.2010.1314

Once through multistage flash desalination: gPROMS dynamic and steady state modeling

Hala Al-Fulaij[a,*], Andrea Cipollina[b], David Bogle[c], Hisham Ettouney[a]

[a]*Department of Chemical Engineering,College of Engineering and Petroleum,Kuwait University, P.O. Box 5969, Safat 13060, Kuwait*
email: engrhala@yahoo.com
[b]*Dipartimento di Ingegneria Chimica dei Processi e dei Materiali, Università di Palermo, Italy*
[c]*University College London, Gower Street, London, WC1E 6BT, UK*

Received 30 April 2009; Accepted 31 January 2010

ABSTRACT

This study focuses on modeling the steady state and dynamic behavior of the multistage flash desalination process (MSF) using gPROMS. This modeling tool allows for simultaneous coding of the system dynamics and steady state performance. In addition, it allows the use of the most efficient solvers for a set of non-linear differential and algebraic equations describing the MSF process. The system model and analysis are based on actual plant data that includes 21 flashing stages and a capacity of 378 kg/s (32,000 m^3/d). The simulated unit is part of a massive MSF installation in Doha, Kuwait. System's dynamic behavior is simulated by a step change in the input values of the main operating parameters, such as the feed flow rate and the top brine temperature. Finally, the analysis of model predictions for both steady-state operation and system dynamics have been compared to actual plant data, showing a good agreement between predicted and measured trends.

Keywords: Desalination; Modeling; Multistage flashing; Steady state; Dynamics; Control

1. Introduction

The MSF process accounts for more than 40% of the entire desalination market [1]. This is achieved through excellent reliability, which is made through continuous process development and accumulation of field experience in design, construction and operation. Part of this progress is achieved by mathematical modeling, which provides an inexpensive tool for understanding process elements, improving system design and troubleshooting, simply through simulation of existing or designed units, and for the development of simple and advanced system controls.

*Corresponding author.

There are several literature studies on modeling of the MSF dynamics [2–12]. All of the dynamic models have similar features and utilize the lumped parameter analysis, where variables are assumed uniform within the flashing stage. In the 1970s and 1980s most of the models were coded using the FORTRAN language. One of the first dynamic models of the MSF process was presented by Glueck and Bradshaw [2]. Drake [3] applied empirical correlations to determine the evaporation rates. Rimawi et al. [4] developed a more comprehensive dynamic model for the once through MSF configuration. The model was solved using a combination of the method of lines and Gears solver of the IMSL library. Their work included limited system analysis; therefore, it is difficult to discern the model efficiency. Husain et al. [5]

used the SPEEDUP code to solve the steady state and dynamics of MSF with brine recycle. In addition, a tridiagonal matrix FORTRAN program is used to obtain the steady-state performance of the system [13]. The SPEEDUP code is used to study system control. Detailed analysis is provided for system dynamics as a function of operating parameters. Calculations are made for long operating times through which new steady conditions are achieved.

Aly and Marwan [6] used a combination of the Newton–Raphson and Runge–Kutta method to solve the MSF dynamic model. The system analysis is limited to very short operating times. This makes it difficult to assess the model efficiency. Thomas et al. [7] coded the MSF dynamic model using C language. The model is very detailed and comprehensive as well as the simulation results. However, review for some of the simulation data reveals that absence of a pressure controller in the last stage results in continuous increase in the brine level.

In the study by Falcetta and Sciubba [8], the CAMEL modular simulator is used to solve the dynamic and steady-state models. Both models were validated against plant and literature data. It is difficult to critique this work because the manuscript does not include details of the mathematical model. However, the authors have used in their model a linear function to simulate the gate height because of lack of knowledge about the interstage dimensions. In reality the gate height fluctuate in non-monotonic manner across the stages. Mazzotti et al. [9] used the LSODA routine to solve the MSF dynamic model. The model includes detailed account of variations in physical properties as a function of temperature and concentration as well as thermodynamic losses. Model results show nonlinear response to variations in steam and seawater temperatures. Tarifa and Scenna [10] used a Delphi 5.0 a computer visual language to simulate the MSF process. The model is comprehensive and the manuscript includes detailed system analysis. Discussion is given for various forms of probable system faults, which might be caused by pumps, valves, heaters, controllers, and heat exchangers.

Shivayyanamath and Tewari [11] used Fortran 95 and the Runge-kutta method to simulate and model the startup characteristics of MSF. The main assumptions in this model are the use of a constant brine holdup in all stages and knowledge of the ejector extraction profile. This reduced the model to simulation of the energy transients within the brine heater and flashing stages. Therefore, it was possible to determine the startup time to reach steady-state conditions.

Bogle et al. [12] developed a comprehensive dynamic model of the MSF. The model details include thermodynamic losses, blow through mechanism, and correlations for the heat transfer coefficients, transport properties, and thermodynamic properties (except for the specific heat of the brine stream, which is assumed constant). The model does not account for demister losses or distillate flashing. The model was applied for an experimental unit and was not validated against real plants.

The above review shows progress in dynamic modeling of the MSF. Part of the progress is found in the continuous attempts of the researchers to obtain a fully comprehensive model that takes into consideration various details within the flashing stage. These details include use of correlations to model thermodynamic losses, physical properties of various streams, and heat transfer coefficients. Other details include account for the vapor blow through phenomenon, release and venting of the non-condensable gases, and control of the brine level in the last stage. These details provide more accurate predictions for the system dynamics and can be used to design new configurations and to understand and troubleshoot the performance of existing systems.

Other elements found in the above review are the methods of solving model equations and also the type of computer codes adopted. Use of efficient and accurate solvers is essential to provide reliable system transients over a long operating period. There are several programming software that can be used to develop a computer code a system model [12]. The most common is FORTRAN, which is difficult to use and generates a rigid code which is difficult to interface with other computer models or simulators. More modern tools such as Matlab, Mathematica, and Visual Basic provide a more efficient platform for development a computer model. However, these software routines have several drawbacks and limitations in development of efficient computer models [17].

gPROMS is an equation-oriented programming tool that provides efficient and accurate modeling platform. gPROMS uses several types of equation solvers (algebraic, ode's, pde's), which simplifies the programming task. Also, it can be easily linked to CFD routines, and physical properties data base. gPROMS allows for logical and conditional statements, which are essential in dynamic simulation and modeling of large systems. Also gPROMS can connect the high level model (Overall system) to the lower level model (flashing stages and different units).

The dynamic model developed in this study takes into considerations all of the essential features and details found in previous literature studies. Also it includes other new details which were not included in the previous models such as the demister effects on the temperature drop, venting line balances across the stages and the distillate flashing in the distillate tray of each stage.

2. The MSF process

The MSF process configuration is constituted by four main parts (see Fig. 1). These are the brine heater, the flashing chambers, feed pre-treatment, and venting line/system. The brine heater has a shell and tube configuration, where the feed seawater flows through the tube side and the heating steam on the shell side. In large plants, the heating steam is introduced through several ports along the length of the heater. This is to ensure uniform temperature distribution within the brine heater. Flashing stages (see Fig. 3) include a brine orifice, brine pool, demister, distillate tray, condenser tubes, and venting tubes. In the flashing stages brine undergoes a flashing process in which vapor is produced at the expenses of the brine sensible heat which is reduced along the stages (how can be seen by the temperature trend). In the upper part of the stage feed seawater flows inside the condenser tubes, where (on the external surface of condenser tubes) the vapor produced in the stages by brine flashing is condensed. As a result, the feed seawater temperature increases due to absorption of the latent heat of the flashed off vapor. On the other side, condensed vapor accumulates and flows in the distillate tray across the stages. The brine leaving the last flashing stage is rejected to the sea. Selected stages are vented to the ejector unit in order to continuously remove and prevent accumulation of the non-condensable gases found in the brine recycle (oxygen, nitrogen, and carbon dioxide). The feed seawater water passes through a coarse screen that removes suspended particles and small organisms. The stream is then treated with a mixture of antiscalent, anticorrosion, antifoaming, and chlorination compounds. Additional details on the MSF process as wells as its features and operating parameters can be found in most of the references cited in this study.

2.1. Mathematical model

The main assumption used in the present MSF dynamic model is related to the lumped parameter formulation for each phase within the stage, such as the flashing brine, the flashed-off vapor and the released non-condensable gases. For example, the flashing brine temperature and salt concentration within each flashing stage are assumed uniform. This assumption is valid because small variations occur in the stream variables within each flashing stage. In addition, it is assumed that heat losses to the surroundings are negligible. This is because estimates for the heat losses account for 2–5%

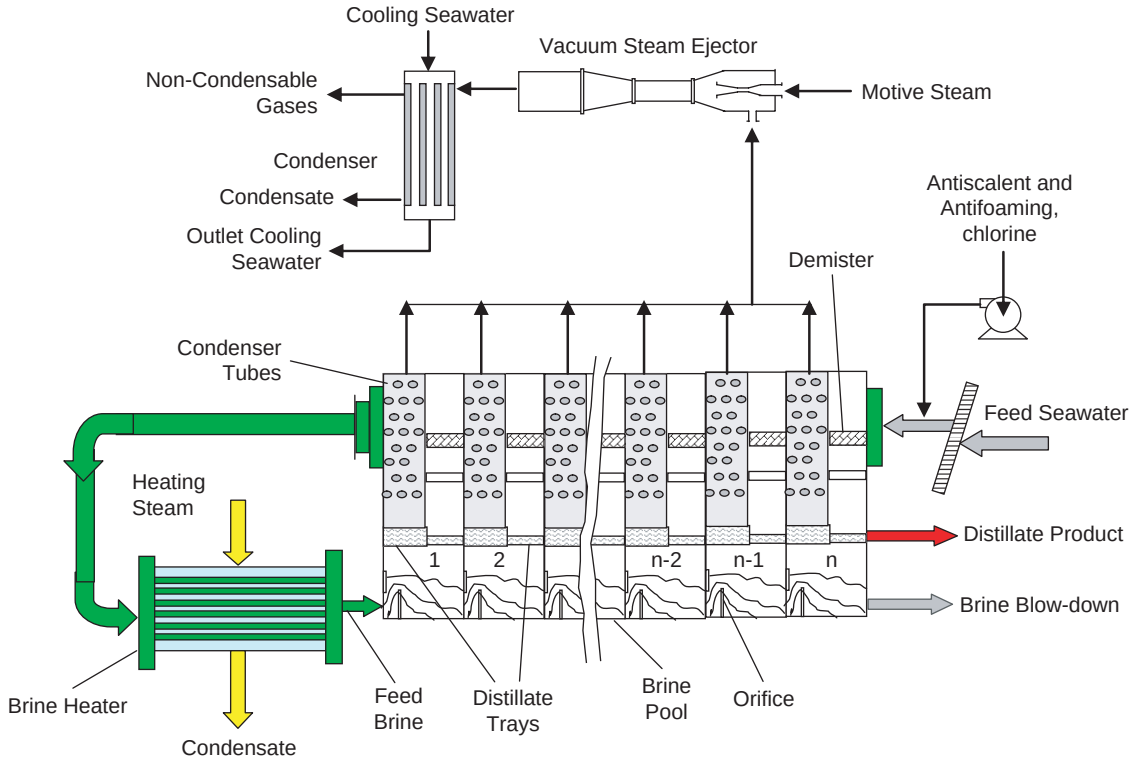

Fig. 1. Schematic of the MSF process.

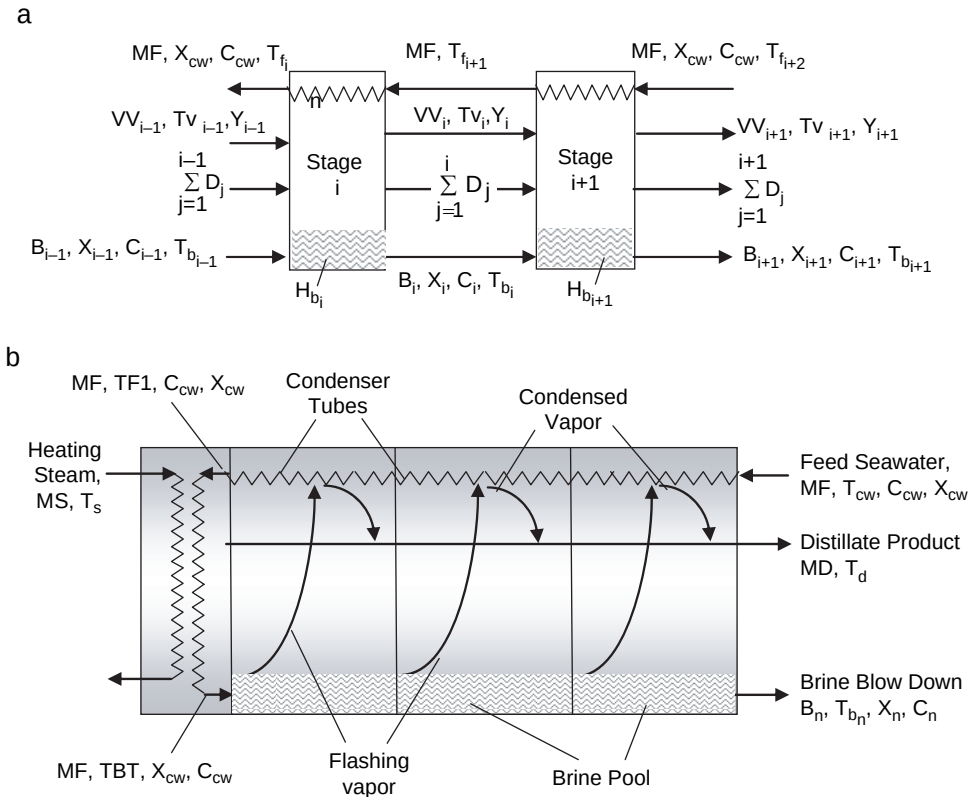

Fig. 2. Process variables in MSF-OT process (a) variables between stages (i) and (i+1) and (b) overall variables.

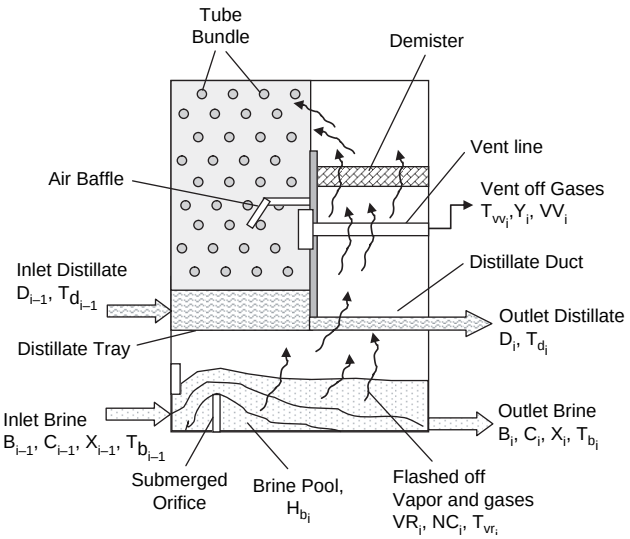

Fig. 3. Stage details and stream variables.

of the total energy of the system [13]. Other assumptions include neglecting demister losses, accumulation in distillate tray, negligible content of non-condensable gases in distillate, and direct venting of non-condensable gases from each stage to the ejector. The dynamic model was constructed in a hierarchical structure. The lower level model includes the algebraic and differential equations which describe the mass and energy balance for individual phases in each flashing stage. The higher level model includes the equations which related the flashing stages to each other to form the process model.

2.2 Stage model

The stage model is formed of a set of dynamic differential balance equations and algebraic balance. Also, the model includes a large number of correlations describing thermodynamic losses, discharge coefficient, and stream physical properties. The dynamic model for each flashing stage (i) includes the following set of differential equations.

Total mass balance of the brine pool:

$$\frac{dM_{b_i}}{dt} = B_{i-1} - B_i - VR_i - NC_i \quad (1)$$

Total mass balance of the vapor space:

$$\frac{dM_{V_i}}{dt} = VR_i + NC_i + D_{i-1} + VV_{i-1} - D_i - VV_i \quad (2)$$

Salt mass balance in the brine pool:

$$\frac{dM_{s_i}}{dt} = B_{i-1} C_{i-1} - B_i C_i \quad (3)$$

Mass balance of the non-condensable gases mass balance in the vapor space:

$$\frac{dM_{nc_i}}{dt} = NC_i + VV_{i-1} Y_{i-1} - VV_i Y_i \quad (4)$$

Mass balance of the non-condensable gases in the brine pool:

$$\frac{dM_{bg_i}}{dt} = B_{i-1} X_{i-1} - B_i X_i - NC_i \quad (5)$$

Enthalpy balance in the vapor space:

$$\frac{dE_{V_i}}{dt} = VR_i\, e_{vr_i} + NC_i\, e_{ncr_i} + D_{i-1}\, e_{d_{i-1}} + VV_{i-1}\, Y_{i-1}\, e_{ncv_{i-1}} + VV_{i-1}\,(1 - Y_{i-1})\, e_{vv_{i-1}} - D_i\, e_{d_i} - VV_i\, Y_i\, e_{ncv_i} - VV_i\,(1 - Y_i)\, e_{vv_i} \quad (6)$$

Enthalpy balance for the brine pool:

$$\frac{dE_{b_i}}{dt} = B_{i-1}\, e_{b_{i-1}} - B_i\, e_{b_i} - VR_i\, e_{vr_i} - NC_i\, e_{ncr_i} \quad (7)$$

In addition, the following algebraic identities and constitutive equations are used in the model.
The distillate tray balance:

$$D_i = D_{i-1} + [VR_i - VV_i(1 - Y_i)] + VV_{i-1}(1 - Y_{i-1}) \quad (8)$$

Mass of brine pool:

$$M_b = \rho_b V_b \quad (9)$$

Volume of brine pool:

$$V_b = A_{st} H_b \quad (10)$$

Mass of vapor space:

$$M_v = \rho_v V_v \quad (11)$$

Volume of vapor space:

$$V_v = A_{st}\,(H_{st} - H_b) \quad (12)$$

Mass of salt in the brine pool:

$$M_s = C\, M_b \quad (13)$$

Mass of gases in the brine pool:

$$M_{bg} = X\, M_b \quad (14)$$

Mass of gasses in the vapor:

$$M_{nc} = Y\, M_v \quad (15)$$

The non-condensable gases stripping rate has been calculated as follows:

$$NC = B(X - X_e)\gamma \quad (16)$$

$\gamma = 0.80$ (efficiency of degassing process)

Specific enthalpy of the inlet brine:

$$e_{b_{i-1}} = Cp_{b_{i-1}} \left(T_{b_{i-1}} - T_{ref}\right) \quad (17)$$

Specific enthalpy of the outlet brine:

$$e_{b_i} = Cp_{b_i} \left(T_{b_i} - T_{ref}\right) \quad (18)$$

Specific enthalpy of the inlet distillate:

$$e_{d_{i-1}} = Cp_{d_{i-1}} \left(T_{d_{i-1}} - T_{ref}\right) \quad (19)$$

Specific enthalpy of the outlet distillate:

$$e_{d_i} = Cp_{d_i} \left(T_{d_i} - T_{ref}\right) \quad (20)$$

Specific enthalpy of the formed non-condensable gases:

$$e_{ncr_i} = Cp_{a_i} \left(T_{vr_i} - T_{ref}\right) \quad (21)$$

Specific enthalpy of the vented non-condensable gases:

$$e_{ncv_i} = Cp_{a_i} \left(T_{vv_i} - T_{ref}\right) \quad (22)$$

Specific enthalpy of the released vapor:

$$e_{vr_i} = Cp_{v_i} \left(T_{vr_i} - T_{ref}\right) + \lambda_{vr_i} \quad (23)$$

Specific enthalpy of the vented vapor:

$$e_{vv_i} = Cp_{v_i} \left(T_{vv_i} - T_{ref}\right) + \lambda_{vv_i} \quad (24)$$

Specific enthalpy of the vapor space:

$$e_{v_i} = \left(Cp_{v_i} \left(T_{v_i} - T_{ref}\right) + \lambda_{v_i}\right)(1 - Y_i) + Cp_{a_i} \left(T_{v_i} - T_{ref}\right) Y_i \quad (25)$$

Total enthalpy of the brine pool:

$$E_{b_i} = e_{b_i} M_{b_i} \quad (26)$$

Total enthalpy of the vapor space:

$$E_{v_i} = e_{v_i} M_{v_i} \quad (27)$$

The demister loss has been calculated from the following relation [14]:

$$\Delta P_p = 3.9(\rho_p)^{0.38}(V_v)^{0.81}(d_w)^{-1.56} \quad (28)$$

The ranges of the experimental variables were V_v (0.98–7.5 m/s), ρ_p (80.32–208.16 kg/m^3), d_w (0.2–.32 mm):

$$T_{v_i} = T_{b_i} - BPE - NEA, \quad (29)$$

where the BPE was calculated based on the correlation obtained by El-Dessouky and Ettouney [14].
Heat balance on the condenser tubes:

$$\begin{aligned} &D_{i-1}(e_{d_{i-1}} - e_{d_i}) + (VR_i - VV_i(1 - Y_i))\lambda_{V_i} \\ &\quad + VV_{i-1}(1 - Y_{i-1})((e_{VV_{i-1}} - e_{VV_i}) + \lambda_{V_i}) \\ &\quad + VV_{i-1}Y_{i-1}(e_{ncv_{i-1}} - e_{ncv_i}) \\ &= MF\, Cp_{b_i}(T_{f_i} - T_{f_{i+1}}) \end{aligned} \tag{30}$$

Heat transfer equation for the condenser tubes:

$$\begin{aligned} &D_{i-1}\left(e_{d_{i-1}} - e_{d_i}\right) + (VR_i - VV_i(1 - Y_i))\lambda_{V_i} \\ &\quad + VV_{i-1}(1 - Y_{i-1})\left((e_{VV_{i-1}} - e_{VV_i}\right) + \lambda_{V_i}) \\ &\quad + VV_{i-1}Y_{i-1}\left(e_{ncv_{i-1}} - e_{ncv_i}\right) \\ &= U_i A_{t_i}\left[\frac{\left(T_{VV_i} - T_{f_{i+1}}\right) + \left(T_{VV_i} - T_{f_i}\right)}{2}\right] \end{aligned} \tag{31}$$

Relation of the heat transfer and number of the condenser tubes:

$$A_t = N_t(\pi D_{to} L_t) \tag{32}$$

All the enthalpies were calculated with respect to liquid water at $T_{ref} = 0$°C. The physical correlations such as brine density, vapor density, specific heat, latent heat and boiling point elevation are available in El-Dessouky and Ettouney [14].

2.3. Non-equilibrium allowance

The following are the correlations used to describe various properties within the stage. The nonequilibrium allowance in the first nine stages with flash box is given by it has been calculated by the following correlation [15]:

$$\begin{aligned} NEA = 166714689.5 \times T_{b_o}{}^{-4.84124} &\left(T_{b_i} - T_{b_o}\right)^{-0.04486} \\ H_b^{1.150576}\, Re_1^{-0.18218}\, Re_2^{0.204095} & \end{aligned} \tag{33}$$

Applicable for 55°C > T_b > 106.55°C and for the rest stages with weir orifice, its correlation is [15]:

$$\begin{aligned} NEA = 6998.338 \times T_{b_o}{}^{-3.13716} &\left(T_{b_i} - T_{b_o}\right)^{-0.02106} \\ H_b^{0.682908}\, Re_1^{0.174489}\, Re_2^{0.042234} & \end{aligned} \tag{34}$$

Applicable for 30.5°C > T_b > 80°C.

Overall heat transfer coefficient [15]:

$$U_o = 0.107309 \times T_v^{0.773247} \times VL^{0.484958}. \tag{35}$$

Applicable for 35°C > T_v > 106.55°C.
Outlet brine flow rate (no-blow through) [16]:

$$\begin{aligned} B_o(i) = Cd(i)\ &(W(i)\ H_g(i)) \\ &\sqrt{ABS\left(2\ \left(P(i) - P(i+1) + (H_b(i) - H_b(i+1))\ g\ \rho_b(i)\right)\rho_b(i)\right)} \\ &*SGN\left(2\ \left(P(i) - P(i+1) + (H_b(i) - H_b(i+1))\ g\ \rho_b(i)\right)\rho_b(i\right) \end{aligned} \tag{36}$$

$$\begin{aligned} V_o(i) = \alpha(i)&\sqrt{ABS\ \left(\rho_v(i)\ \left(P(i) - P(i+1)\right)\right)} \\ &SGN\ \left(\rho_v(i)\ \left(P(i) - P(i+1)\right)\right) \end{aligned} \tag{37}$$

where (i) referes to the stage under study and (i + 1) refers to the next stage.
When blow through starts [16]:

$$\begin{aligned} B_o(i) = Cd(i)\ &\left(W(i)\ H_b(i)\right) \\ &\sqrt{ABS\left(2\ \left(P(i) - P(i+1) + (H_b(i) - H_b(i+1))\ g\ \rho_b(i)\right)\rho_b(i)\right)} \\ &SGN\left(2\ \left(P(i) - P(i+1) + (H_b(i) - H_b(i+1))\ g\ \rho_b(i)\right)\rho_b(i\right) \end{aligned} \tag{38}$$

$$\begin{aligned} V_o(i) = &\left(\alpha(i) + W(i)\ \alpha'\left(H_g(i) - H_b(i)\right)\right) \\ &\sqrt{ABS\left(\rho_v(i) * \left(P(i) - P(i+1)\right)\right)} \\ &SGN\left(\rho_v(i)\ \left(P(i) - P(i+1)\right)\right) \end{aligned} \tag{39}$$

For the last stage, outlet pressure is fixed and a control loop is inserted to control the brine level in the last stage [16]:

$$K_{c\_b} = 0.9\, B_i(1)/0.07 \tag{40}$$

$$B_o(21) = 0.9\, B_i(1) + K_{c\_b}\left(H_b(21) - H_{sp}\right) \tag{41}$$

The discharge coefficient is calculated from calculation based on real plant data [15]. For the flash box stages:

$$\begin{aligned} Cd = 0.49 \times &\left(\frac{H_g}{\left(\frac{\Delta P_{1-2}}{\rho_b\ g}\right) + H_{bi}}\right)^{-0.058508} \\ &\times \left(\frac{v_1}{v_2}\right)^{0.187808} \times \left(\frac{\rho_b}{\rho_m}\right)^{-0.234325} \times \left(\frac{H_1}{H_2}\right)^{0.1997656}. \end{aligned} \tag{42}$$

Applicable for 55°C > T_{bo} > 106.55°C

And for the weir gate stages [15]:

$$Cd = 0.139938 \times \left(\frac{H_g}{\left(\frac{\Delta P_{1-2}}{\rho_b\, g} \right) + H_b} \right)^{0.147156} \times \left(\frac{v_1}{v_2} \right)^{1.33021} \times \left(\frac{\rho_b}{\rho_m} \right)^{0.36234} . \quad (43)$$

Applicable for $30.5°C > T_{b_o} > 80°C$.

2.4. Brine heater model

The brine heater heat balance is

$$M_{stm}\ \lambda_{stm} = MF\ Cp_b\ (TF1 - TbT) \quad (44)$$

The Plant gain output ratio (GOR)

The plant gain output ratio is defined as the mass flow rate ratio of the distillate product to heating steam

$$GOR = MD/M_{stm} \quad (45)$$

3. Results and discussion

The dynamic simulation is performed for the plant parameters shown in table 1. Figs. 4–6 illustrates the system transients after changing the seawater flow rate from 4048 to 4010 kg/s [18] and then changing it back to 4048 kg/s. Figs. 7–9 illustrates the system response after changing the top brine temperature (TBT) from 91°C to 89°C [18] and then restoring its value to 91°C.

Figs. 4–6 show variations in the system variables upon the decrease in the feed flow rate from 4048 kg/s to 4010 kg/s and then restoring the original condition of feed flow rate of 4048 kg/s. Decrease of the feed flow rate results in drastic reduction in the brine level in all stages. As shown, most of the system variables, which includes the condensate flow rate, salinity, stage pressure, stream temperature, and brine flow rate, increase or decrease monotonically across the stages. The variations in all of these variables are intimately related to the system temperature, which obviously decreases monotonically from the hot to the cold end of the plant. As a result, the flashing rate, the brine temperature, the vapor temperature, the condensate rate, the brine flow rate, and the stage pressure all would decrease between the hot and cold ends of the plant. On the other hand, the brine concentration would increase between the hot and cold ends of the plants.

Fig. 6 shows the system dynamics for the plant gain output ratio (GOR) which is defined as the mass flow rate ratio of the distillate product to heating steam [14]. As shown it reaches a steady-state value of 7.45. This is well below industrial standards and is caused by the large difference between the outlet temperature of the feed seawater from stage 1 and the top brine temperature (TBT). The plant GOR can be increased through the increase in the number of condenser tubes, which results in the increase of the condenser heat transfer area and the outlet temperature of the feed seawater from stage 1.

Figures 7–9 show variations in the system variables upon step change in the top brine temperature (TBT) from 91°C to 89°C and then restoring the original conditions of 91°C. Decrease in the top brine temperature reduces the flashing range which reduces the amount

Table 1
Parameters used in simulation of MSF-OT system.

Parameter	Value	Units
Number of stages (*n*)	21	
Stage width (Wst)	17.66	m
Stage length (Lst)	3.150	m
Stage height (Hst)	4.521	m
Number of condenser tubes (Nt)	1410	
Condenser tubes outer diameter (ODt)	0.0445	m
Condenser tubes inner diameter (IDt)	0.04197	m
Brine level set point in the last stage (Hst)	0.668	m
Top brine temperature (TBT)	91	°C
Intake sea water flow rate (MF)	4027	kg/s
Intake sea water salinity (C_{cw})	40000	ppm
Intake sea water temperature (T_{cw})	37.7	°C
Steam temperature (T_{stm})	111	°C
Venting line pressure	7000	Pa
Non condensable gases concentration in feed seawater (C_{cw})	18.1	mg/kg (ppm)

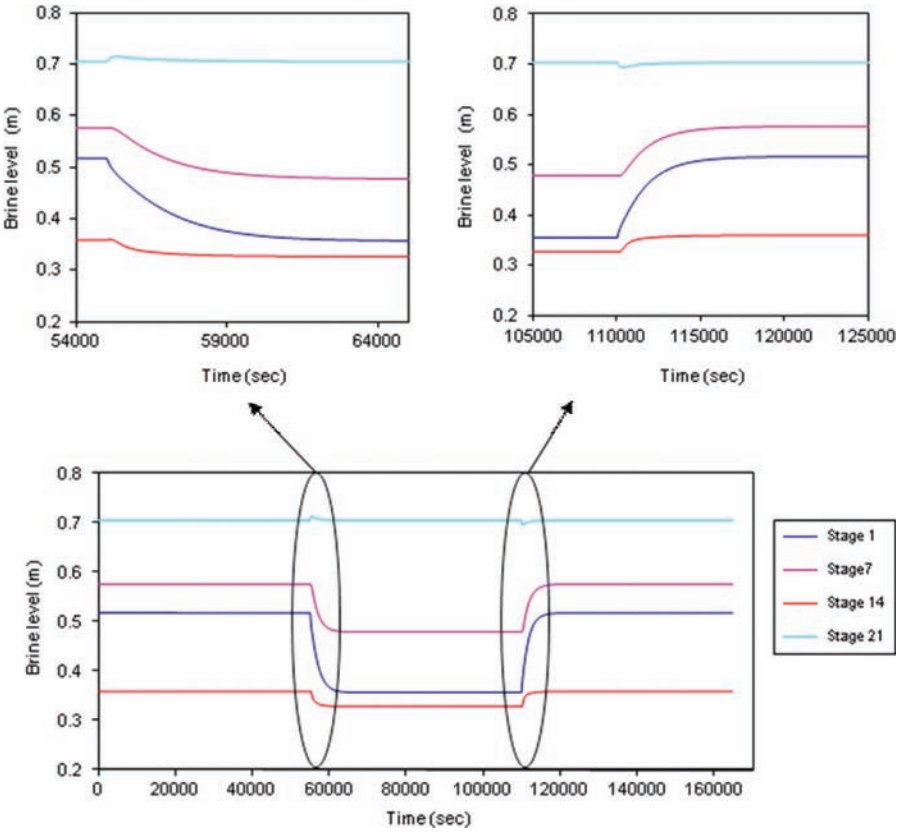

Fig. 4. Dynamics of the brine level in stages 1, 7, 14 and 21 for step changes in the feed seawater flow rate (MF).

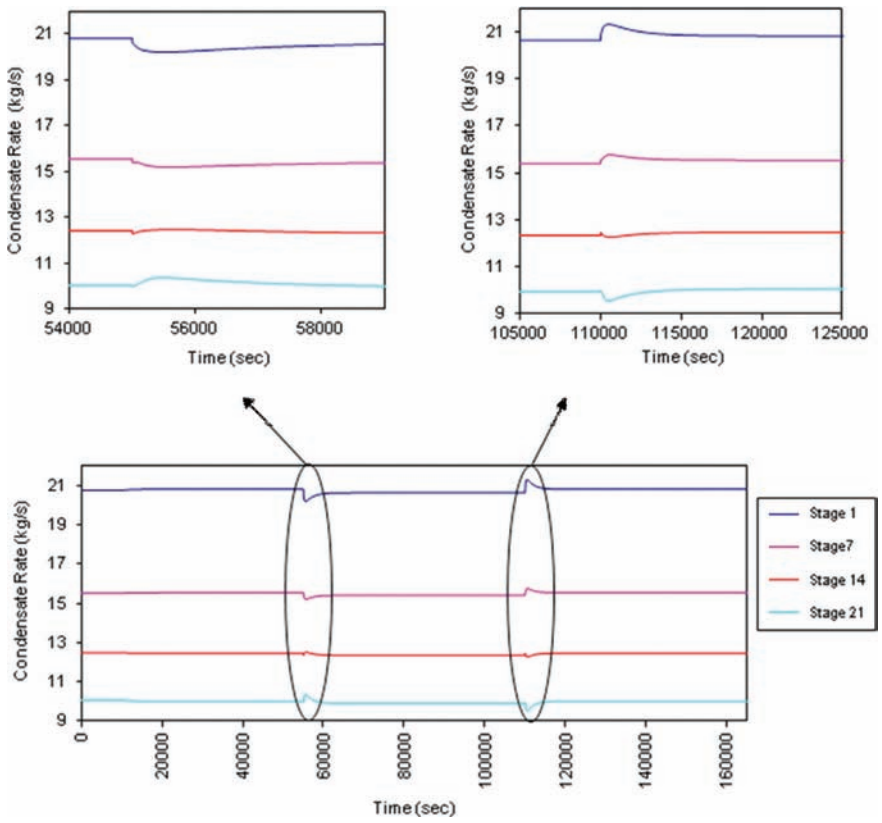

Fig. 5. Dynamics of condensate rate in stages 1, 7, 14 and 21 for step changes in the feed seawater flow rate (MF).

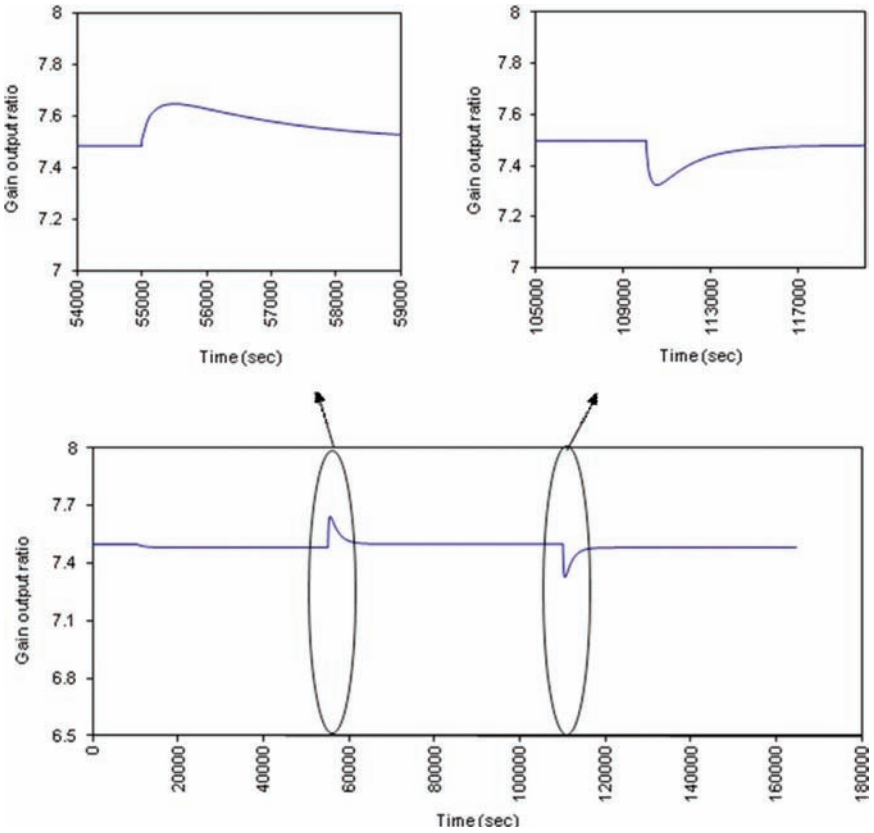

Fig. 6. Dynamics in GOR in stages 1, 7, 14 and 21 for step changes in the feed seawater flow rate (MF).

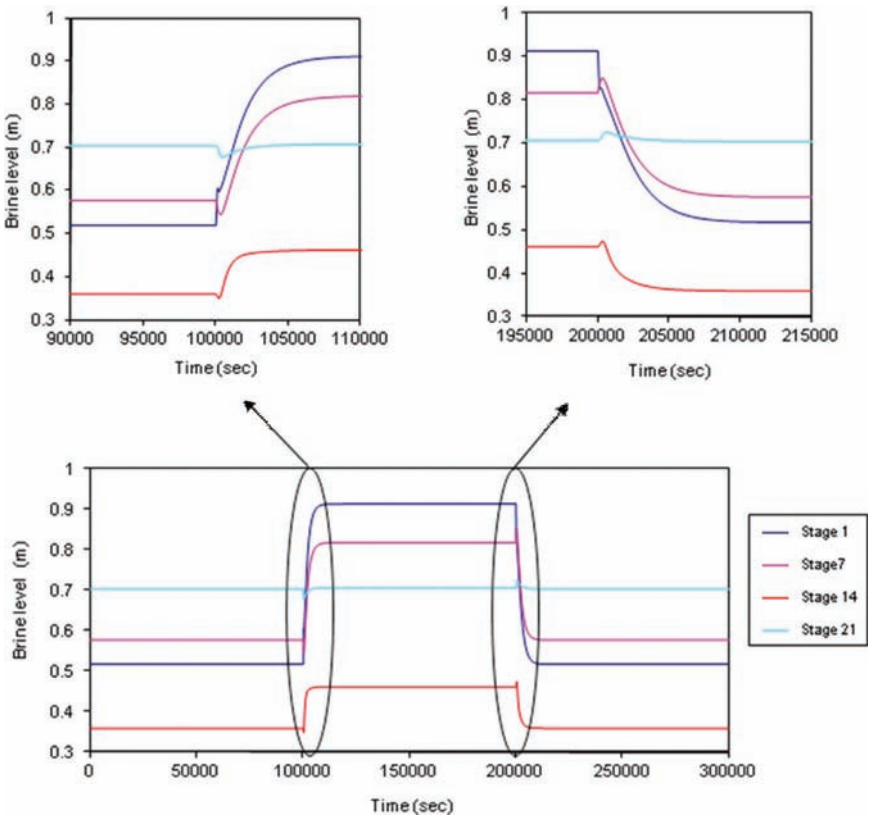

Fig. 7. Dynamics of the brine level in stages 1, 7, 14 and 21 for step changes in the Top brine temperature (TBT).

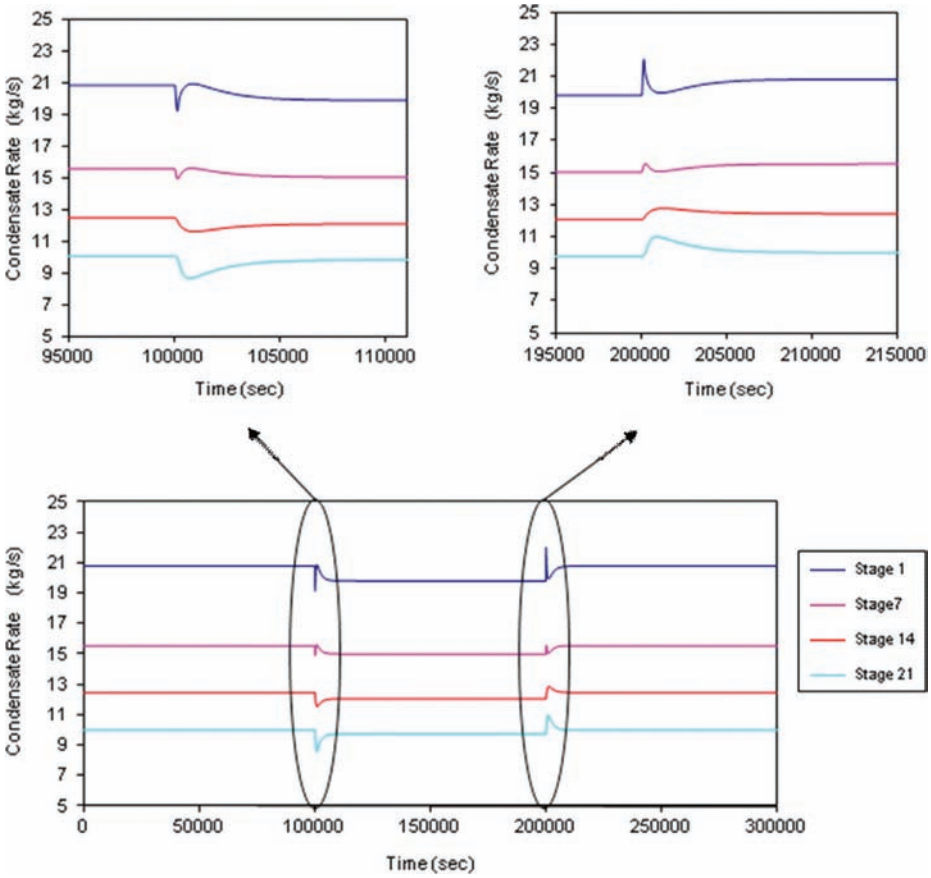

Fig. 8. Dynamics of the condensate rate in stages 1, 7, 14 and 21 for step changes in the top brine temperature (TBT).

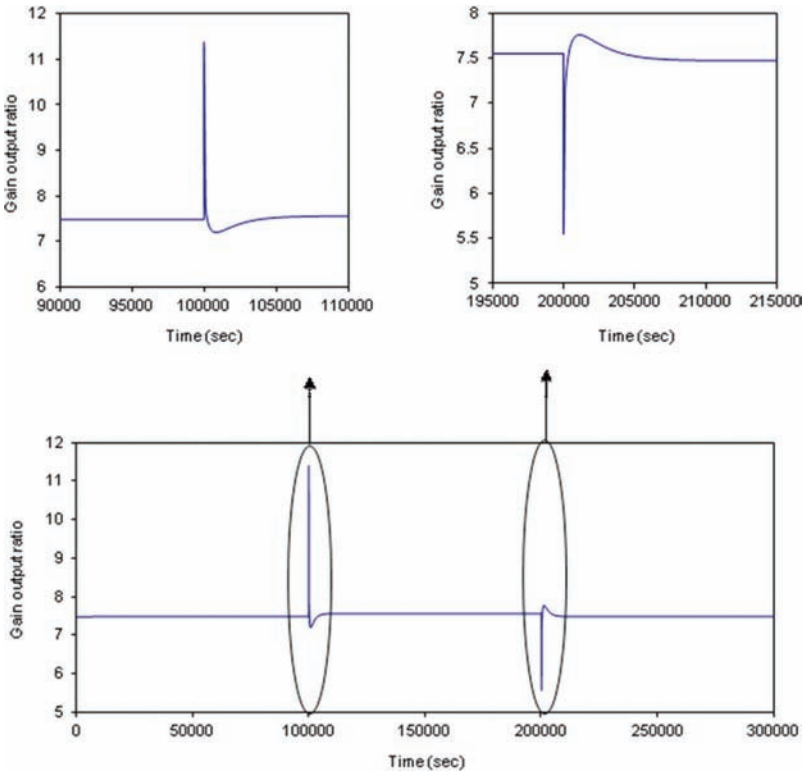

Fig. 9. Dynamics of GOR in stages 1, 7, 14 and 21 for step changes in the top brine temperature (TBT).

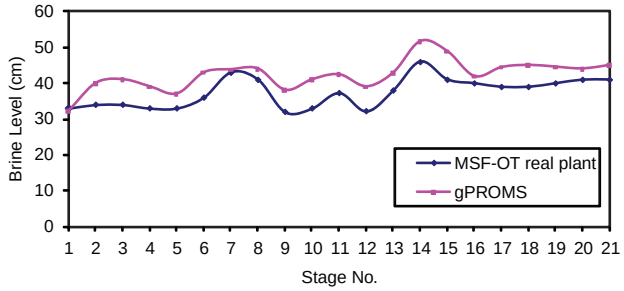

Fig. 10. Non-monotonic behavior in the brine level in the stages of MSF-OT plant.

of vapor formed. This will results in the increase of the brine level in all stages and reduction in the condensation rate. As shown, the top brine temperature (TBT) has more drastic effect on the brine level especially in the first stage. This is because of the rapid and large change that occurs in the temperature and pressure of the stage. Other system variable are also affected, but, at a lesser magnitude. This is illustrated by dynamic variations in the condensate rate and the plant GOR. The trends in both variables indicate slight variations in the steady-state values across the stages.

As shown in Fig. 10, non-monotonic behavior in the brine level. This is because the brine height depends on several parameters, which may result in its increase or decrease. For example, the brine height increases with the decrease of the discharge coefficient, stage pressure, temperature drop per stage, and gate height. A monotonic increase should have been observed in the brine height because of the monotonic decrease in the system temperature. However and because of the unequal variations across the stages, the brine height changed in an uneven manner.

3.1. Comparison of model predictions and plant data

Comparison of the model predictions is made against field data for existing MSF plants (see table 1). The comparison was for steady-state and dynamic data, which includes variations in the flow rate, salinity, and temperature profiles of the brine stream across the stages. For the steady-state comparison, results are shown in Fig. 11. As shown, good agreement is obtained between model predictions and the plant data, especially for the brine flow rate and salinity, where the errors did not exceed 0.4% for both variables. On the other hand, the relative error in predicting the stage temperature is limited to a maximum of 0.62%.

For the dynamic data comparison, the comparison was made for data collected from daily operation, where small disturbances occur in operating parameters. These include the top brine temperature, the brine recycle flow rate, and intake seawater temperature. Summary of the plant operating parameters, which are made every four hours for a period of 24 h, are shown in table 2. As shown, small disturbances are found in this data, which

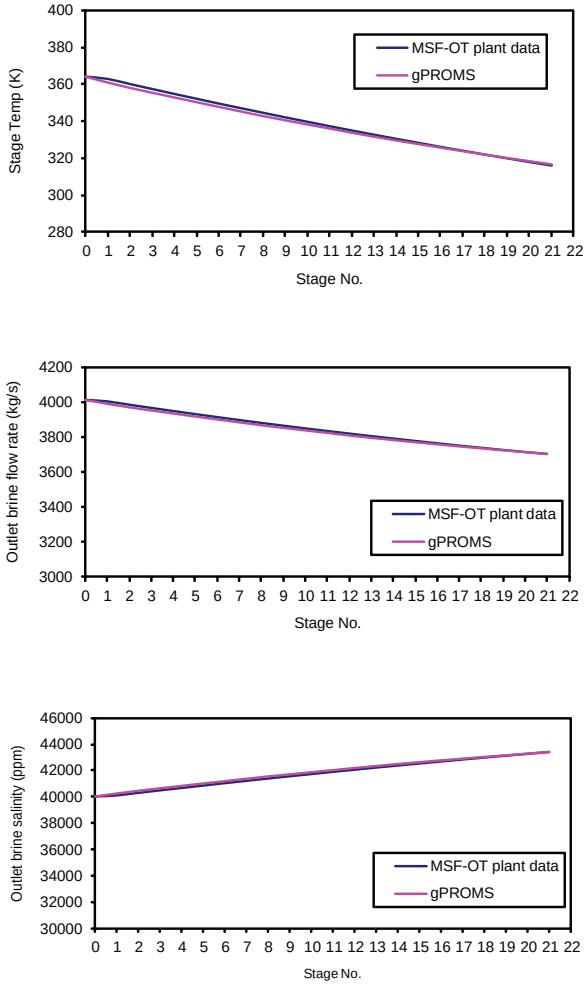

Fig. 11. Comparison of gPROMS predictions and the field data for stage profiles of flow rate, salinity, and temperature of the brine stream.

Table 2
Disturbances occurring in MSF-OT real plant over a period of 24 hours.

Time (hr)	Top brine Temp. (C)	Mfeed (Kg/hr)	Inlet seawater (C)
0	91.3	14 491 000	37.7298
4	91.4	14 574 000	37.8169
8	91.1	14 491 000	37.8016
12	91.1	14 574 000	37.8749
16	91	14 450 000	37.8601
20	91.3	14 491 000	37.6854
24	91.5	14 533 000	37.7061

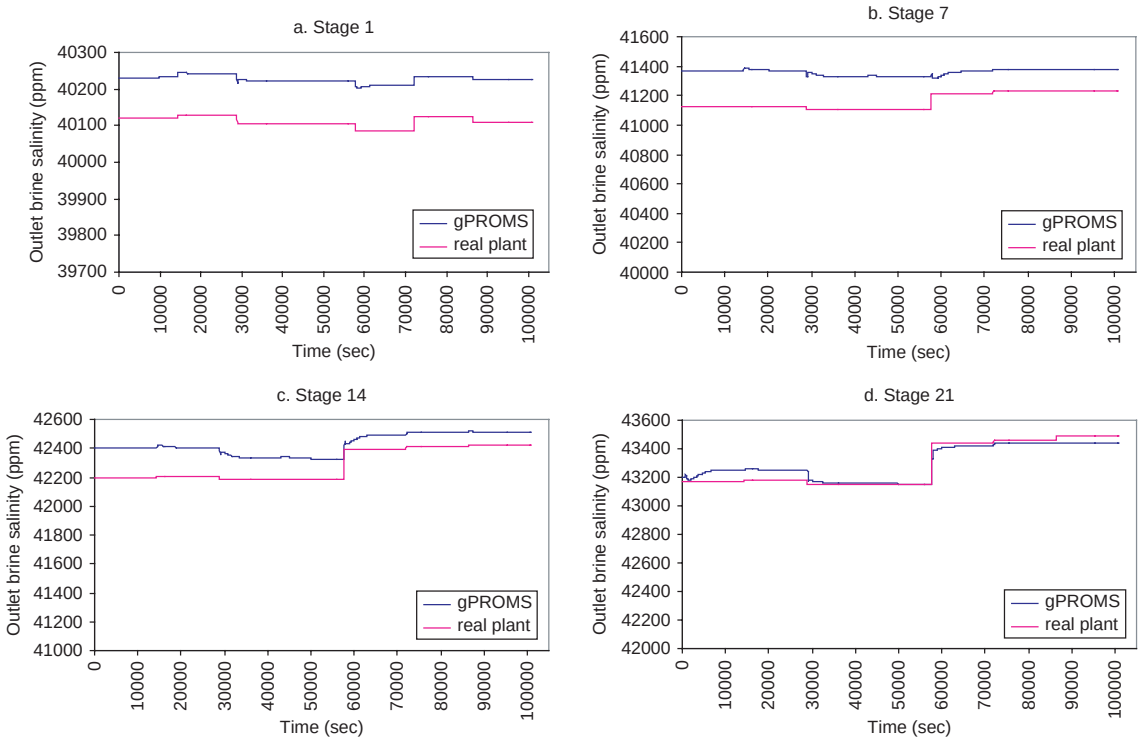

Fig. 12. Comparison of gPROMS predictions and the field dynamic data for stage profiles of salinity of the brine stream.

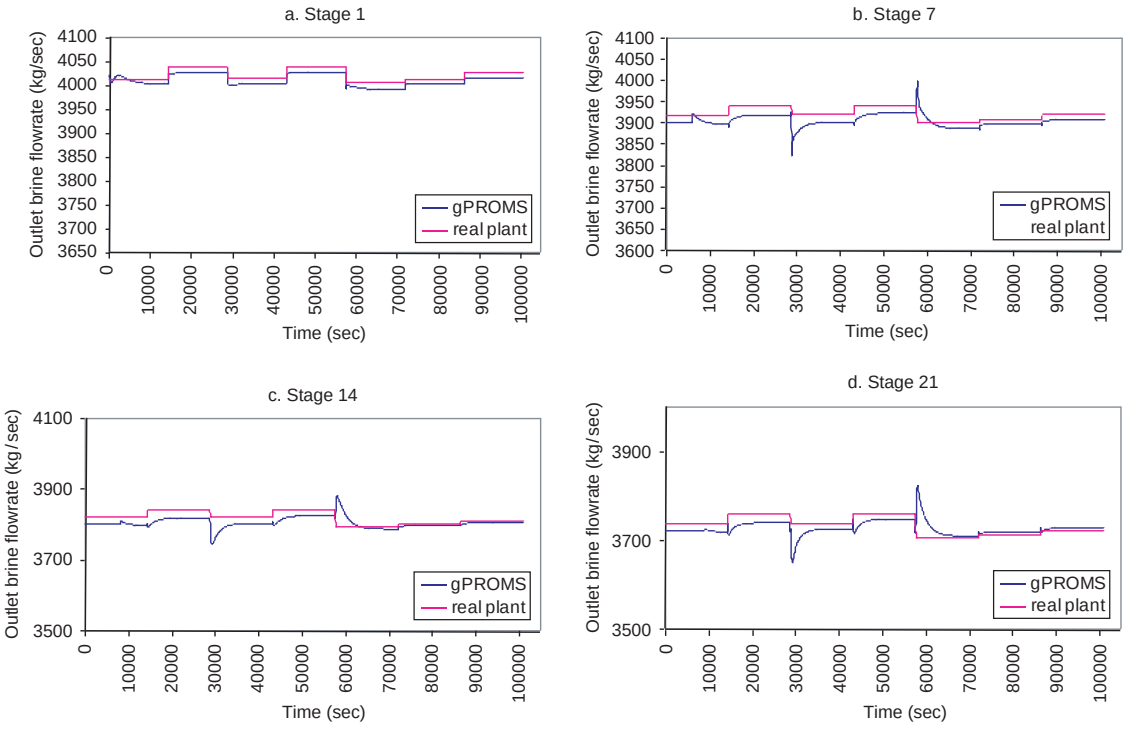

Fig. 13. Comparison of gPROMS predictions and the field dynamic data for stage profiles of flowrate of the brine stream.

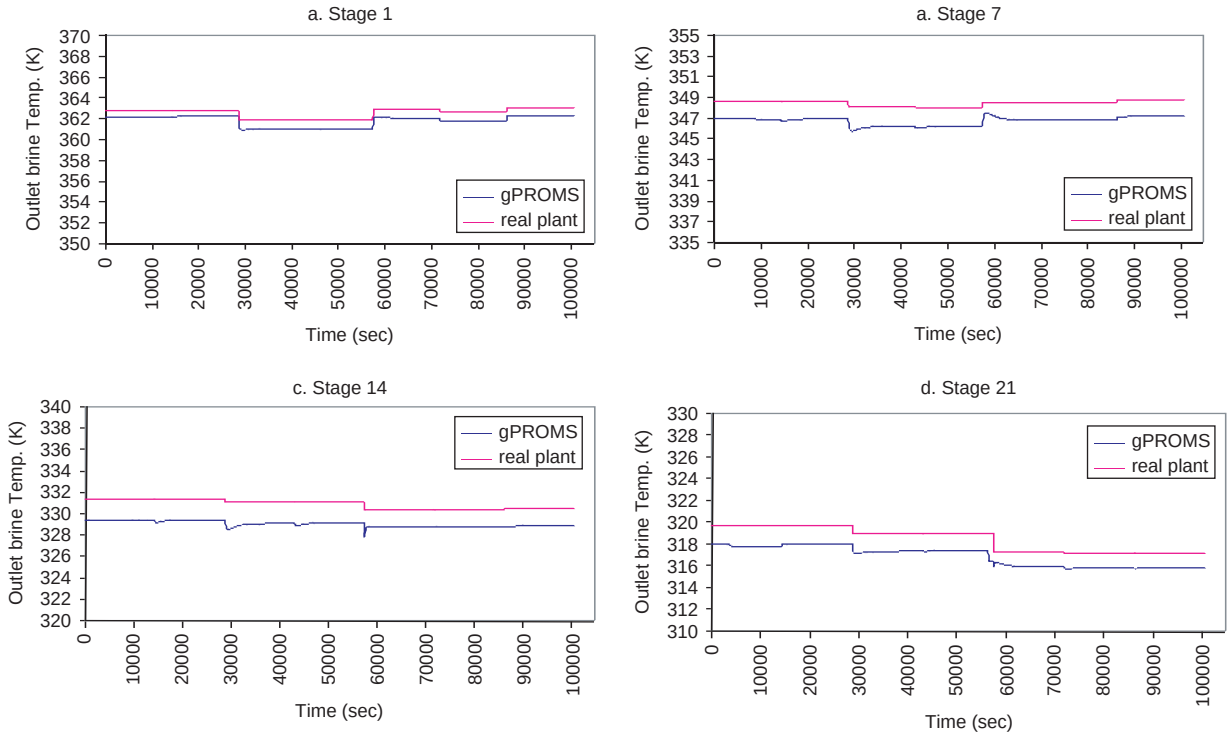

Fig. 14. Comparison of gPROMS predictions and the field dynamic data for stage profiles of Temperature of the brine stream.

are caused by daily fluctuations in solar insolation and heating steam pressure. The solar insolation affects the intake seawater temperature and the heating steam pressure affects the top brine temperature. As a result, small changes are made in the brine recycle flow rate in order to maintain the plant at the desired design conditions.

Comparison of model predictions and plant data include the flow rate, salinity, and temperature profiles of the brine stream across the stages. Results are shown in Figs. 12–14. As shown, good agreement is obtained between model predictions and the plant data, especially for the stage temperature where the errors did not exceed 0.81%. On the other hand, the relative error in predicting the brine flow rate and salinity is limited to a maximum of 2.5% for the brine flow rate and 0.63% for the brine salinity.

4. Conclusions

A comprehensive lumped parameter model is presented for design and simulation of the steady-state and dynamic behavior of the MSF process. The model is solved using the gPROMS software, which provides very efficient tools for solving the non-linear set of differential and algebraic equations constituting the MSF model. The developed model includes most of the essential features found in previous literature studies such as thermodynamic losses, and vapor blow through. In addition, the model takes into account distillate flashing, venting of non-condensable gases, demister losses, calculation of the plant GOR, and design of the brine heater.

The plant dynamics are analyzed for a base case set of conditions, which corresponds to actual plant data. The dynamic profiles show that the plant approaches steady-state conditions within a period of one to two hours. This is consistent with previous literature data and available plant data. Further system analysis is performed for the cases of imposing a sequence step variations in some of the operating conditions, which includes the intake seawater flow rate and the top brine temperature. The step changes are limited to values below 5%. All results of this test show that the plant maintained stable operation and it was possible to recover original operating conditions.

Comparison of the model predictions and actual field data has been performed for both steady-state and dynamic operations. A very good agreement is obtained between predictions and field data with small differences which did not exceed 2.5%.

References

[1] The 19th IDA worldwide desalting plant inventory, International desalination association, Topsfield, MA, USA, 2006.
[2] A.R. Glueck and W. Bradshaw, Proc. 3rd International Symposium on Fresh Water from sea, 1 (1970) 95–108.
[3] F.A. Drake, Chapter 2.1 Measurements and control in flash evaporator plants, Desalination, 59 (1986) 241–262.
[4] M.A. Rimawi, H.M Ettouney and G.S. Aly, Transient model of multistage flash desalination, Desalination, 74 (1989) 327–338.
[5] A. Husain, A. Woldai, A. AI-Radif, A. Kesou, R. Borsani, H. Sultan and P.B. Deshpandey, Modelling and simulation of a multistage flash (MSF) desalination plant, Desalination, 97 (1994) 555–586.
[6] N.H. Aly and M.A. Marwan, Dynamic behavior of MSF desalination plants, Desalination, 101 (1995) 287–293.
[7] P.J. Thomas, S. Bhattacharyya, A. Petra and P. Rao, Steady state and dynamic simulation of multi-stage flash desalination plants: A case study, Comp. Chem. Eng., 22 (1998) 1515–1529.
[8] M.F. Falcetta and E. Sciubba, Transient simulation of a real multi-stage flashing desalination process, Desalination, 122 (1999) 263–269.
[9] M. Mazzotti, M. Rosso, A. Beltramini and M. Morbidelli, Dynamic modeling of multistage flash desalination plants, Desalination, 127 (2000) 207–218.
[10] E. Tarifa and J. Scenna, A dynamic simulator for MSF plants, Desalination, 138 (2001) 349–364.
[11] S. Shivayyanamath and P.K. Tewari, Simulation of start-up characteristics of multi-stage flash desalination plants, Desalination, 155 (2003) 277–286.
[12] D.L. Bogle, A. Cipollina and G. Micale, Dynamic modeling tools for solar powered desalination process during transient operations, Proceedings of the NATO advanced research workshop on Solar Desalination for the 21st Century, L. Rizzuti, H. Ettouney, and A. Cipollina (eds), NATO Security through Science Series, Springer, Dordrecht, The Netherlands, 2007.
[13] A.M. Helal, M.S. Medani, M.A. Soliman and J.R. Flower, Tridiagonal matrix model for multi-stage flash desalination plants, Comp. Chem. Eng., 10 (1986) 327–342.
[14] H.T. El-Dessouky and H.M. Ettouney, Fundamentals of Salt Water Desalination, Elsevier, Amsterdam, The Netherlands, 2002.
[15] H. Al-Fulaij, Analysis of MSF flashing chambers, Master thesis, Kuwait University, Kuwait, February (2002).
[16] A. Cipollina, Experimental study and dynamic modelling of multi stage flash desalination units, PhD thesis, 2004–2005.
[17] I.D.L. Bogle and B.E. Ydstie, 2004, Model based process equipment design. Computer Aided Process and Product Engineering, D.L. Puigjaner and G.Heyen (eds), Elsevier.
[18] N. Al-Deffeeri, Chemical Section Head, Doha West Power station, Ministry of Water and Electricity, Personal communication, 2009.

Nomenclature

A	Area, m^2.
B	Flow rate of flashing brine between stages, kg/s.
BPE	Boiling point elevation,°C.
C	Salt concentration, kg/m^3
Cd	Discharge coefficient
C_p	Specific heat at constant pressure, kJ/kg °C
D	Flow rate of the distillate between stages, kg/s.
D_{to}	Outer diameter of condenser tubes, m
d_w	demister wire diameter, mm
e	Specific enthalpy, kJ/kg
E	Total enthalpy, kJ
g	gravity acceleration, m/s^2
H_b	Brine height, m
$H1,H2$	Flash box dimension (m)
Hg	gate height, m
H_{sp}	set point for the brine height in the last stage, m
$K_{c\text{-}b}$	Proportional controller gain, kg/s m.
L	Length of condenser tubes, m
M	Total mass, kg
MF	Intake seawater flow rate, kg/s
N	Number of the condenser tubes
VR	Mass flow rate of released vapor stream, kg/s
NC	Mass flow rate of non-condensable gases, kg/s
NEA	Non-equilibrium allowance, °C
P	pressure, kPa
Re_1	Reynolds number at orifice gate
Re_2	Reynolds number at brine level height
t	Time, s
T	Temperature, °C.
TF1	Brine temperature entering the brine heater, °C
TBT	Top brine temperature, °C
U	Overall heat transfer coefficient, kW/m^2 °C.
VV	Mass flowrate of vented stream, kg/s
V	Volume, m^3
Vv	Vapor velocity across the demister , m/s
v_1	Velocity (m/s^2) = $B_o(i\text{-}1)$ / [$\rho b(i\text{-}1)\ h_b(i\text{-}1)$]
v_2	Velocity (m/s^2) = $B_o(i)$ / [$\rho b(i)\ h_b(i)$]
VL	brine velocity in the tube bundle, m/s
W	Stage width, m.
X	Mass fraction of gases in the brine
Y	Mass fraction of non-condensable gases in the vented vapor
ΔPp	demister pressure drop, Pa

Greek Letters

λ	Latent heat of vaporization, kJ/kg.
ρ	Mass density, kg/m^3.
ρ_p	demister packing density, kg/m^3.
γ	Efficiency of degassing process
α	venting line orifice discharge coefficient.
α'	gas phase discharge coefficient

Subscripts

a	air
b	Brine
b_i	Brine stream flowing in the condenser tubes
b_o	Brine stream flowing out the condenser tubes
bg	Gases in the brine
e	Equilibrium
f	Brine stream flowing inside the condenser tubes
nc	Non-condensable gases
ncr	Released non-condensable gases
ncv	vented non-condensable gases
s	Salt
st	Flashing stage
stm	steam
t	Condenser tubes
v	Vapor
vr	Released vapor
d	distillate
i	stage number i
vv	vented stream